

Operation of the *Spektr-R* Orientation System

M. M. Lisakov^a, S. M. Voinakov^c, A. S. Syrov^b, V. N. Sokolov^b, D. A. Dobrynin^b, M. A. Shatsky^b,
R. A. Kamaldinova^b, V. V. Sosnovtsev^b, N. V. Ryabogin^b, T. B. Vyunitskaya^b, and E. N. Filippova^c

^a *Astro Space Center, Lebedev Physical Institute, Russian Academy of Sciences, Leninskii pr. 53, Moscow, 119991 Russia*
e-mail: lisakov@asc.rssi.ru

^b *Moscow Experimental Design Bureau MARS, Moscow, Russia*
e-mail: office@mokb-mars.ru

^c *Lavochkin NPO (Science and Production Corporation), Khimki, Moscow oblast, Russia*
e-mail: voinakov@laspace.ru; flen@laspace.ru

Received December 16, 2013

Abstract—Errors in pointing and sustaining *Spektr-R* are estimated based on the data of star sensors and an angular velocity vector meter, and the calculated values are compared with the observed values. It has been indicated that the achieved pointing accuracy is significantly better than the required accuracy and is independent of the number of star sensors used for this purpose; finally, the stabilization parameters correspond to the anticipated parameters. The original method for processing adjustment observations of the space radio telescope in the 1.35-cm range used to find a systematic deviation of 2.5' of the telescope real electric axis from the nominal angular position has been described.

DOI: 10.1134/S0010952514050086

INTRODUCTION

The *Spektr-R* onboard control system (OCS) is designed in order to maintain spacecraft functioning in the working orbit and to observe cosmic radioemission sources with the space radio telescope (SRT).¹ These aims can be achieved if the specified accuracy and spacecraft orientation limitations are satisfied. Scientific data are transmitted directly to ground control and tracking stations during observations through a moving high-gain communication antenna (HGCA) of the spacecraft High-Data-Rate Communication radio link.

The main OCS functions are as follows: to control the angular motion of the spacecraft and the motion of the center of mass; to control the functioning of the spacecraft adjacent systems, units, and aggregates (ASs); to form telemetry parameters in order to estimate the OCS state and process data (obtained when the scientific equipment was adjusted during a flight) on the ground; to calculate the mass center motion based on the initial conditions specified on the ground; and to calculate the angular orientation of HGCA one-axis homing in order to point HGCA at the specified ground station based on this procedure.

OCS operates in the following main regimes: constant solar-pointing (CSP); inertial pointing (IP), i.e., triaxial spacecraft stabilization relative to the specified schedule position according to AVVGM information

(see below) with or without AVVGM drift stellar monitoring, delta-velocity maneuver (DVM), and spinning for the following passive gyroscopic stabilization (GS) of spacecraft.

The set of typical flight operations can be performed in OCS. By combining these operations and specifying their parameters on the ground, it is possible to construct various spacecraft angular maneuvers during a flight, including maneuvers performed in order to calibrate control units and determine the relative angular position of control and scientific units.

Pointing is specified and determined relative to the equatorial coordinate system: the inertial coordinate system (ICS) of standard epoch J2000.0. The schedule position of the spacecraft sight coordinate system (SCS) is specified as quaternion with respect to ICS in command-programming information (CPI) that comes from the Earth or is autonomously formed by OCS varying in time based on CPI data. Spacecraft and SRT coordinate systems are determined in [2] and [3], respectively.

OCS includes (a) the onboard digital computational system (ODCS) with a control and switching unit; (b) power supply units; (c) control units (CUs), i.e., an angular velocity vector gyroscopic meter (AVVGM) with four measuring channels developed at Kuznetsov NII PM; star sensors (SSs), i.e., three star sensors AD-1; sun-position indicators, i.e., two sun-position indicators SDP-1; and (d) inertial end organs, i.e., the complex of attitude-control reaction

¹ <http://www.asc.rssi.ru/radioastron/documents/rauh/en/rauh.pdf>

wheels (RWs) with four RWs designed at the Research Institute of Control Units.

In addition, as end organs, OCS uses stabilization and correction engines (SEs and CEs, respectively). Stabilization engines are used to extinguish angular velocities after the spacecraft separation, CSP construction, RW unloading, spacecraft spinning, and spacecraft stabilization in the rotation channel during DVM with the help of CE in order to perform small delta-velocity maneuvers and during the suppression of abnormal situations.

After the spacecraft is inserted into the final orbit, the automatic cyclogram for controlling the initial orbit segment is triggered. This cyclogram is used to arrest angular separation velocities and to transit spacecraft into the CSP regime, which provides the orientation of the solar panel (SP) toward the Sun in the initial position after deployment in order to create energy income and necessary thermal regimes. When the cyclogram terminates and the current orientation is determined with SSs, the spacecraft is transferred into the autonomous regime, i.e., its orientation is maintained in the IP regime when all onboard systems operate normally and mission tasks (MTs) are anticipated in order to perform the next procedures.

The spacecraft operation program is constructed so that disturbances of the spacecraft angular stabilization and its mass center motion should be eliminated during interferometer or adjustment observations. Therefore, the orbit correction, RW unloading, and SP reorientation are assigned outside of the observation periods.

Control of Spacecraft Pointing during Scientific Observations Based on AVVGM and SS Signals

The following requirement to the pointing parameters are specified in the requirements specifications (RS): spacecraft SCS pointing errors (3σ) without errors in the relative adjustment of CU and SCS device coordinate systems (DCSs) along each of the SCS axes should be not more than $18''$; the stabilization should deviate from the average value by no more than $\pm 2.5''$ on any 120 s interval; the angular velocities of stabilization should be no more than $2 \times 10^{-4} \text{ deg s}^{-1}$ along the SCS Y and Z axes and $5 \times 10^{-4} \text{ deg s}^{-1}$ along the X axis.

The spacecraft orientation is controlled according to the principles of corrected strapdown INS. The orientation accuracy specified in RS is achieved by using AVVGM and SS signals in order to control orientation and by the functioning of the OCS information support subsystem in the regime of continuous stellar monitoring (CSM). In the CSM regime, two SSs continuously operate and the spacecraft orientation parameters calculated based on AVVGM signals at a stellar data arrival rate of 0.5 Hz are corrected.

The AVVGM drift calibration is specified from the mission control center (MCS) by introducing the cor-

responding MT to spacecraft. The planned periodicity of the AVVGM drift calibration depends on the stability of systematic drifts and, on average, occurs once a week. If scientific observations are performed at a constant orientation and are rather prolonged (6–18 h), AVVGM drifts can be calibrated against a background of these observations.

The AVVGM scale factors and the relative angular position of AD-1 and AVVGM were calibrated by the Moscow Experimental Design Bureau MARS once during the initial stage of spacecraft operation. This procedure made it possible to eliminate discrepancies in the CU coordinate system caused by the inaccuracy of ground-based measurements and by the effect of overpressures during the injection of the spacecraft into orbit.

SPEKTR-R ORIENTATION ERROR DURING SCIENTIFIC OBSERVATIONS

The main components responsible for the *Spektr-R* orientation total error are as follows:

Δ_1 is the determination errors of the spacecraft orientation parameters immediately after the next data occurrence from SS (at an interval of 2 s) with regard to the inclusion of these data in processing by the Kalman filter;

Δ_2 is the orientation parameter calculation errors based on AVVGM signals within a 2-s interval between data occurrence from SS due to uncompensated AVVGM drifts;

Δ_3 is calculation errors in the orientation parameter based on AVVGM signals caused by the signal noise components;

Δ_4 is errors in the stabilization system.

The presented errors are independent, since they originate independently. We study the levels of these errors, reducing them to equivalent errors of the spacecraft orientation determination and control. The effect of the remaining factors on the spacecraft orientation accuracy is eliminated based on the calibration of the AVVGM scale factors and CU relative angular position.

Errors of Determining Parameters for Spacecraft Orientation Based on SS Data

The star sensor error includes three components, i.e., a noise component; a systematic component that manifests as a periodic component when a star image moves over the CCD matrix, and a systematic component including the constant and LF components.

The third error component was eliminated as a result of the SS calibration during the initial flight state with the telemetry data processing on the ground. According to the calibration results, CPI that is used to correct the output data of the star sensor is introduced into the spacecraft.

The second error component is determined as a microdistortion, i.e., the systematic error whose value depends on the star image position relative to the CCD matrix screen-type pattern [4]. In the presence of angular velocity, this error manifests as a pseudorandom periodic value. If the spacecraft schedule angular motion relative to ICS is absent and the stabilization amplitudes are small, this component becomes an inherent systematic error.

During stellar sighting at a low spacecraft angular velocity (15–30 arcsec s⁻¹), the Kalman filter, which is used to calculate the stellar orientation, eliminates the noise and periodic components of the SS error. Otherwise, the filter only eliminates the noise error component, and the second component becomes systematic, since it is not registered when the star image does not cross the CCD matrix. Thus, the star pointing error at a low angular velocity is smaller than when a constant SCS orientation relative to ICS is specified.

OCS is responsible for the spacecraft star pointing relative to ICS through the orientation of the SS measuring coordinate system, which is virtual and is identified through SS output data.

The star pointing errors considered below are the orientation errors of measuring CSs of calibrated adjusted star sensors relative to ICS.

The upper estimate (δ) for the resultant star pointing error of SS measuring CS can be represented as $\delta = \alpha + f$, where f is the filtering error due to the first and second components of the SS error (the second SS error component is not filtered during stellar sighting at a constant SCS orientation relative to ICS) and α is the upper estimate of the contribution to the star pointing error caused by the SS systematic error component. Parameter f is calculated as $f = 3\sqrt{Sp(L)}$, where $L(3 \times 3)$ is the covariance matrix of the Euler rotation vector element error transforming the orientation of ICS of the leading AVVGM basis, calculated by the filter, into true ICS in the situation when the SS systematic error is absent. Parameter α is represented as $\alpha = \varepsilon k$, where ε is the error of the compensation for the third SS error component.

If the angular velocity is 15 arcsec s⁻¹, this parameter is about 4". When stellar sighting is performed at a constant SCS orientation relative to ICS, the second SS error component reaching 20" is added to this value. Coefficient k dependent on the relative star configuration in a frame used to calculate pointing is determined as $k = \sqrt{R/2}$, where $R = -Sp(I^{-1})$, $I = \sum_{i=1}^N \hat{s}^{(i)} \hat{s}^{(i)}$.

Here, N is the number of stars in one frame used to calculate pointing, and $\hat{s}^{(i)}(3 \times 3)$ is skew symmetric matrix corresponding to the projection column of a unit vector pointed to the i -th observed star.

The estimate of the pointing error through a trace of the covariance matrix of the Kalman filter state vec-

tor error on the three-month interval is presented in Fig. 1. This estimate includes all systematic errors of star identification on spacecraft, including the errors related to the relative position of observed stars, e.g., to small angular distances between stars. The star pointing error can be considered an integral resulting characteristic of the star sighting session. At each instant, the error value depends on the number of stars in the SS field of view and their relative position. The pointing error estimate through a trace of covariance matrix of the Kalman filter state vector error is not more than 3".

Errors in the Stabilization System

The integral component is included in the control law during the scientific observations. According to TMI data, the statistical error is reduced to 0° in this case, and the angular oscillation amplitude along the SCS X , Y , and Z axes is not more than 0.33", 0.72", and 0.36", respectively. The angular velocity oscillation amplitude along the SCS X , Y , and Z axes is not more than 0.000025, 0.00003, and 0.00002 deg s⁻¹, respectively.

SPEKTR-R ORIENTATION ERROR DURING SCIENTIFIC OBSERVATIONS

The total orientation error (Σ) can be defined as $\Sigma = \sum_{i=1}^n \Delta_i$, where Δ_i are the independent partial error components ($i = \overline{1, n}$).

In this case, the total error variance can be determined through the values of partial variances as follows:

$$\sigma_{\Sigma}^2 = \sum_1^n \sigma_{\Delta_i}^2 \text{ or } 3\sigma_{\Sigma} = \sqrt{\sum (3\sigma_{\Delta_i})^2}.$$

The contribution of the independent partial factors to the total error upper limit of the spacecraft orientation in the CSM regime is as follows: $\Delta_1 = 3''$, $\Delta_2 = 0.004''$, $\Delta_3 = 0.9''$, and $\Delta_4 = 0.72''$. The upper limit of total error of spacecraft orientation sustaining along each of the SCS axes is

$$3\sigma_{\Sigma} = \sqrt{3^2/3 + 0.004^2 + 0.9^2 + 0.72^2} = 2.3''.$$

Conditions of OCS Operation to Meet Spektr-R Orientation Accuracy Requirements during Scientific Observations

The above estimates indicate that, respect to the spacecraft orientation, the RS requirements with sustaining accuracy during the scientific observations are met when the following conditions are satisfied:

(1) The residual AVVGM drifts along each SCS axis are maintained due to periodic calibrations at a level of no more than 0.002 deg h⁻¹.

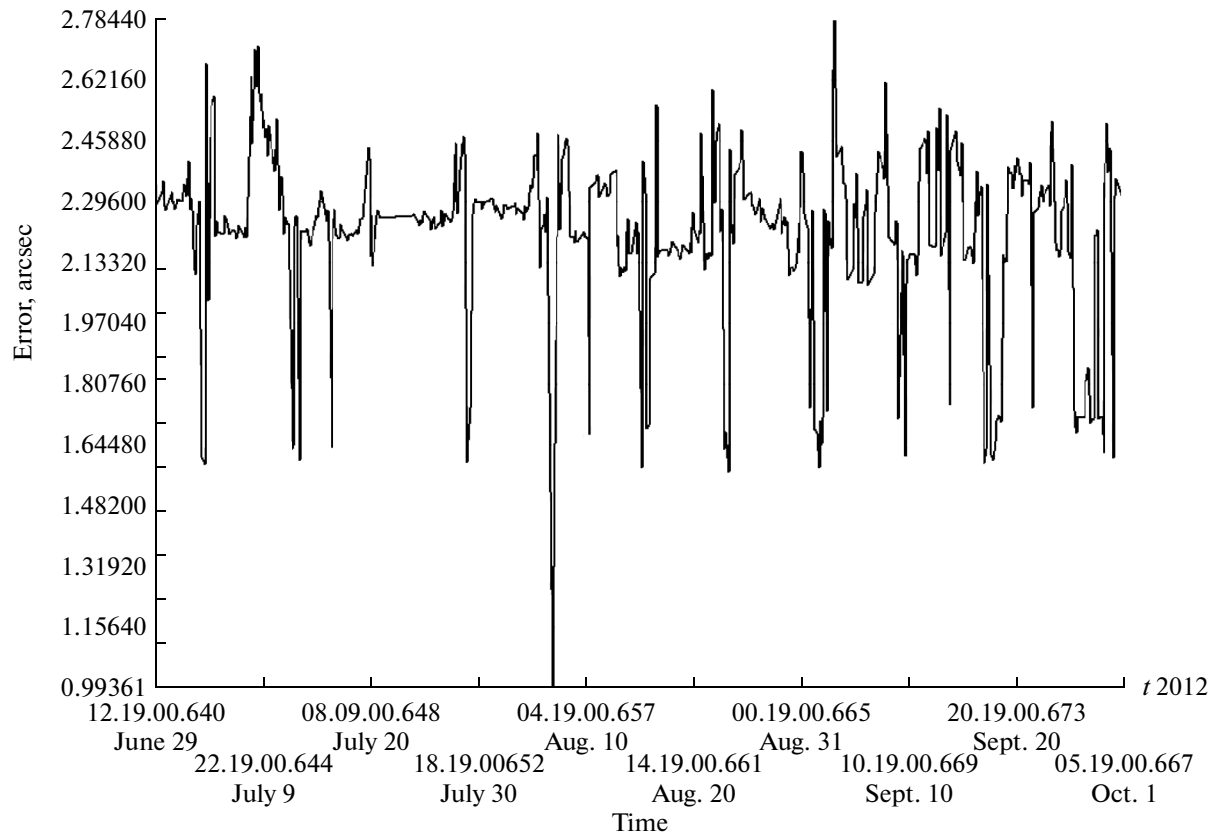


Fig. 1. Time variations in the calculated orientation error (arcsec).

(2) The spacecraft orientation relative to ICS is determined in the CSM regime using two SSs. The orientation accuracy needed for scientific observations is achieved at the second–fourth minute after the CSM regime onset.

(3) The relative angular adjustment of CU and the SRT electric axis was performed.

(4) Disturbances caused by the rotation of solar panels are absent during the scientific observations, and the disturbances caused by moving HGCA turnings are within tolerable limits.

(5) For each scientific observation session, an SS pair of three OCS sensors should be selected, taking into account that these sensors are not illuminated by the Earth and the Moon (see [3]) and the total information content of the starry heavens is maximal in the sensor fields of view.

DATA USED TO ANALYZE THE SRT POINTING AND SUSTAINING ACCURACY

The first SRT observations in the scope of the RadioAstron project were performed in November 2011. More than 900 interferometric observations and several tens of adjustment observations were performed by the moment.

The interferometric observations are mostly performed using the onboard program of the telemetry frame formation, according to which data on the current SCS orientation come from OCS into the telemetry system approximately once per minute. Typically, the duration of the session varies from 40 min to 1 h. Thus, the angular position along each SCS axis was measured at least 40 times during most interferometric observations. Data on the direction of only the SCS X axis were used and analyzed for the present paper.

Special adjustment observations during which SRT operates in the single dish mode are regularly performed in order to determine SRT parameters. Radiometric output data from one or two receivers in both polarizations and 1-s data on orientation are stored during these observations. After the adjustment observations, data from a storage unit (SU) are transmitted to the Earth through the telemetry system.

During the adjustment observations, the SRT electric axis scans a small area on the celestial sphere according to one of several prescribed programs. Scanning is performed by scans implemented by the spacecraft rotation around the Y or Z axes. Several passes can be performed over each scan. A transition zone is used to pass from scan to scan. The characteristic trajectories of the SCS X axis in equatorial coordinates during the adjustment observations are pre-

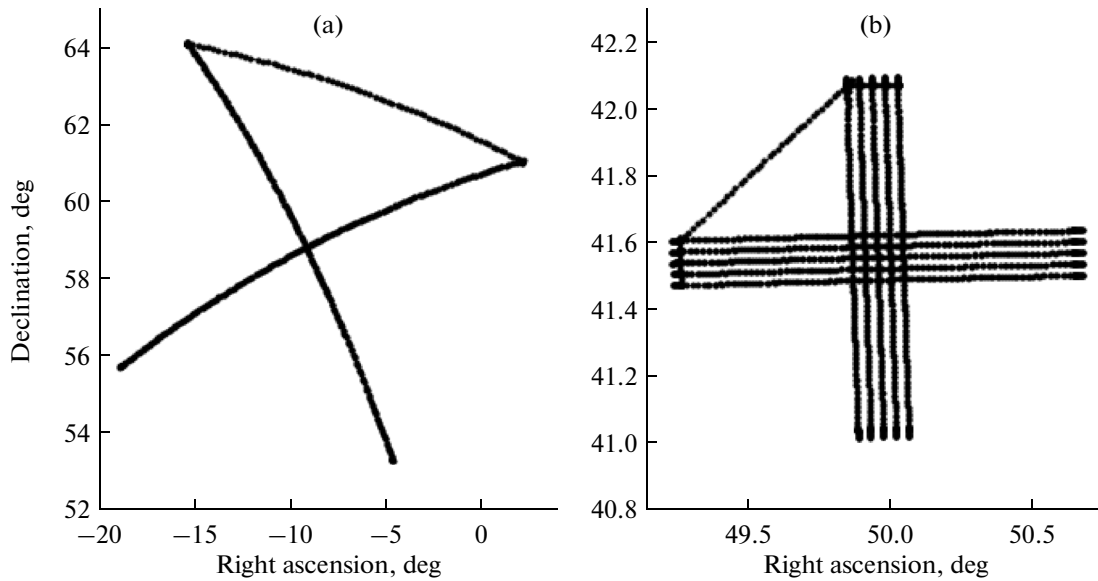


Fig. 2. *X* axis trajectory during the adjustment observations (a) in the 18- and 92-cm ranges (the scan length 5°, the spacecraft rotation velocity 36 arcsec s⁻¹) and (b) in the 6- and 1.35-cm ranges (the scan length 1°, the distance between scans 2.5', the spacecraft rotation velocity 18 arcsec s⁻¹). Five scans around the SCS *Y* axis and five scans around the *Z* axis (two passes in each scan).

sented in Fig. 2. Each data point obtained from telemetry information corresponds to a certain direction of the SCS *X* axis.

DATA PROCESSING AND ANALYSIS

Orientation quaternions (*c*₁, *c*₂, *c*₃, *c*₄) in telemetry information (TMI) can be used to calculate equatorial coordinates of the orientation (right ascension α , declination δ) of all three SCS axes using the known formulas.² For the SCS *X* axis, these equations are

$$\alpha = \arctan \frac{2(c_1c_4 + c_2c_3)}{c_1^2 + c_2^2 - c_3^2 - c_4^2}$$

$$\delta = \arcsin(2(c_2c_4 - c_1c_3)).$$

Data of the interferometric and adjustment observations were processed differently. A difference in the coordinates between the SCS *X* axis orientation and source was studied, and the distribution of parameters of this difference were estimated when the interferometric sessions were processed. Thus, the total spread of points along each coordinate α , δ characterizes the spacecraft stabilization system operation accuracy, and the difference between the median value of the *X* axis position during the observation session and the true position of the observed source in the sky characterizes the orientation determination uncompensated error (pointing accuracy). Special software and a database that included SRT pointing coordinates for all observations were developed in order to perform this analysis. Figure 3 shows the SRT pointing data for one of the first interferometer sessions (rafs02). Each point

corresponds to one position of the *X* axis according to the telemetry data (the time step is 60 s). The position of the studied source (0212 + 735) is marked. The total spread of points is not more than 1.5''.

When the adjustment sessions were analyzed, not only the *X* axis coordinates but also radiometric responses of receivers were taken into account, which made it possible to study the dependence of the receiver output power on SRT pointing coordinates. This unique SRT possibility gives it a great advantage over ground telescopes during adjustments.

Point sources are certainly the best calibrators for the radio telescope adjustment. The brightest objects observed with SRT (Crab Nebula, Cassiopeia A) are resolved in the 1.35 cm band, and the number of

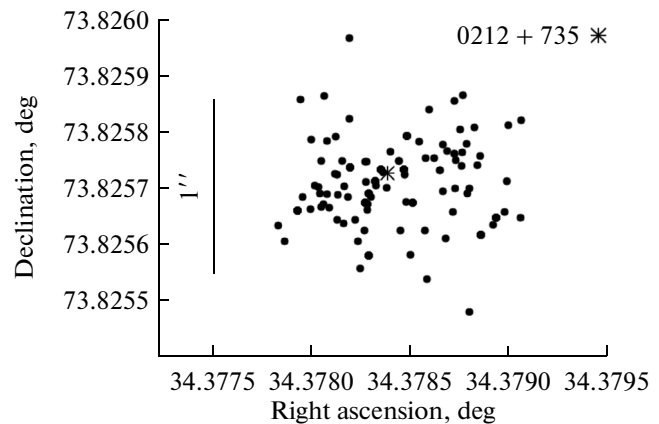


Fig. 3. Typical variations in the orientation of the *X* axis during the interferometer observations. Vertical segment corresponds to an angular distance of 1''.

² <http://en.wikipedia.org/wiki/Quaternion>.

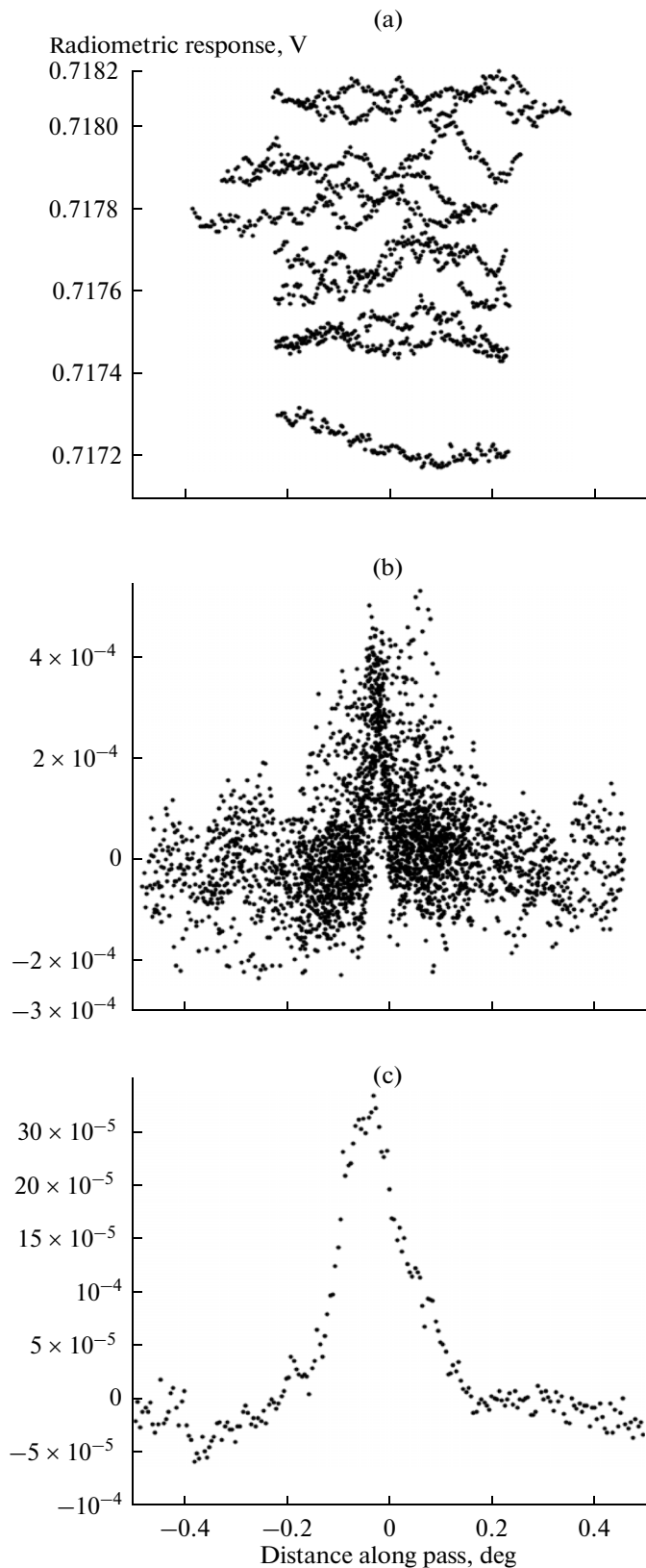


Fig. 4. Receiver radiometric responses of 1.35 cm during the rotation around the Z axis when the adjustment was performed according to the scheme presented in Fig. 2b during different filtering stages.

accessible point objects is small since the SRT sensitivity is low in this waveband [1]. The largest number of adjustment observations in the 1.35 cm band was performed for radio galaxy 3C84. We faced two difficulties: first, responses of radiometric outputs from 3C84 in the 1.35 cm band are often not visible above system noise; second, the system temperature is rather highly variable (the LF fluctuation amplitude is larger than the response to a source by an order of magnitude) during standard 1.5-h adjustment observations.

To overcome these difficulties and increase the adjustment accuracy, we developed an original method that includes the following stages of data processing:

(1) A median filter was applied to time variations in a radiometric signal $S(t)$. The filter parameters were selected so that HF noise (including responses to a source) would be eliminated. Thus, we obtained a smoothed signal $M(t)$ that describe only large-scale variations in the system temperature. A smoothed signal was subtracted from an initial one $S(t) - M(t) = C(t)$. As a result, the obtained pure signal was free of large-scale variations in the system temperature.

(2) It was necessary to average the data in order to improve the signal-to-noise ratio. For this purpose, we divided data into individual passes over a source. We considered the dependence of the radiometric response $C(r)$ on the pointing distance with respect to the source along a pass. Since the source is a point, each pass $C_i(r)$ is the cross-section of the SRT beam pattern. Assuming that the beam can be represented by two-dimensional Gaussian $D(\alpha, \delta)$, we anticipated that the dependence of the response to a source on distance can be approximated by Gaussian $D_i(r)$ along each pass. In this case we independently considered passes in perpendicular directions (rotation around the Y and Z axes) and passes in opposite directions about the same axis (clockwise and counterclockwise around the Y and Z axes). Finally, we obtained four data sets, studied independently, each included four or five (depending on the scanning scheme) passes over a source in the same direction. Response amplitudes in different passes are different; however, the response width and the position of maxima should be identical based on the assumption that the beam is Gaussian. Since an analysis was aimed to determine the position of maxima, we averaged responses in each data set. Figure 4a presents unfiltered $S(r)$ dependences. Each curve is the dependence of the receiver response on the distance along a scan. Five scans with two passes each are shown in Fig. 4a. Since the receiver gain drifted, the average values of the receiver response are different in each pass. Figure 4b shows several filtered passes $C(r)$, and Fig. 4c presents a signal averaged over all passes $A(r)$. The distance from the calculated position of the observed source measured along a scan is plotted on the abscissa (the anticipated response maximum should be at point 0).

(3) The resultant averaged signal $A(r)$ was approximated by Gaussian. Among the Gaussian parameters, we only used the width at a half maximum level and the

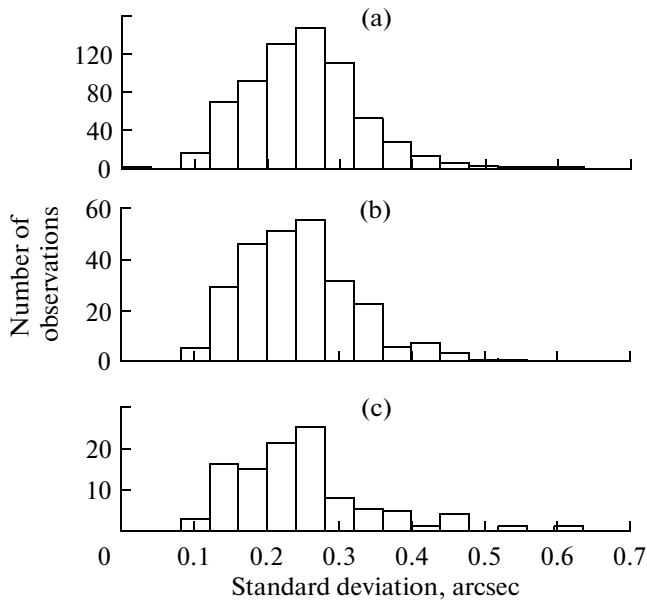


Fig. 5. Pointing accuracy (orientation determination) distribution (a) for all interferometer observations in the project and for the observations performed in 2013 using (b) two SSs and (c) one SS.

position of a maximum. For each adjustment, we finally obtained four widths of the response to a source (which corresponds to the beam pattern width when a point source is observed) and four response maximum positions according to the scheme described above. The Gaussian fitting errors were accepted as total errors of these parameters.

RESULTS

Correction for the Position of the SRT Electric Axis

During the adjustment measurements (scanning of the $1^\circ \times 1^\circ$ area) in the 1.35 cm band, it was found that coordinates of the maxima of the responses to a source differ from source coordinates. In other words, the real SRT electric axis (the SRT beam pattern maximum) differs from the SCS X axis. Owing to the specific features of the SRT beam pattern in the 1.35 cm range [1], we only managed to reliably find the deviation along the SRT Y axis. In this case, the deviation has two components, i.e., the constant component and the variable component dependent on the spacecraft rotation direction.

The deviation constant component is $2.5'$ and can be explained by, e.g., deformations that took place during the spacecraft launch and SRT unfolding. In this waveband, the beam pattern size measured along the Y axis is $6'$. Thus, if the axis deviation is ignored, the sensitivity of SRT and the ground–space interferometer would decrease approximately twofold and by a factor of approximately 1.4, respectively.

The deviation variable component is $1'$ and is always directed against SRT rotation, thereby causing

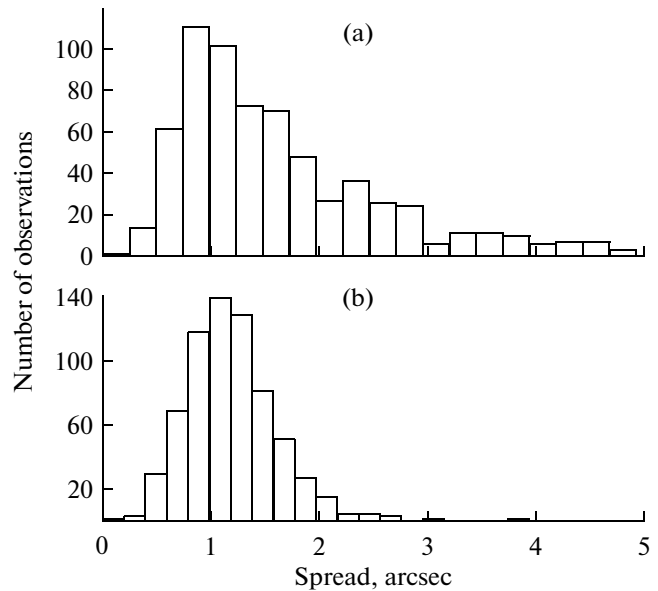


Fig. 6. Distribution of the spread of SRT pointing points during the interferometer observations of (a) right ascension and (b) declination.

the displacement of the maximum of the response to a source along the motion or, what is the same, the delay of the maximum arrival time as compared to the calculated time. The variable component of the deviation can be partially explained by the delay in the receiver integrating circuit (for more detail, see the discussion in [1]).

The presence and stability of the deviation constant component were verified during the adjustments performed in November 2011–January 2012. A correction of $2.5'$ was introduced into the standard software for calculating SRT pointing on December 15, 2011.

SRT Pointing Accuracy

Processing the data of SRT pointing during the interferometric sessions made it possible to obtain the distributions of the SRT electric axis standard deviations (1σ) from the direction toward a source (with regard to the $2.5'$ correction) for all observations up to October 2013 (about 900 observations). This standard deviation characterizes the accuracy of SRT pointing to a specified source. The standard deviation distributions over the angular distance between the pointing point and a source are presented in Fig. 5a. The median value of the distance standard deviation is $0.24''$ for all observations, which is much better than the required orientation determination accuracy. The standard deviation is mostly not more than $0.4''$.

After January 4, 2013, the SRT orientation was performed using only one SS in some observations. We compared the pointing accuracies when the procedure was performed using two (Fig. 5b) and one (Fig. 5c) SSs using only the data for 2013. The SRT pointing accuracies obtained using one (the median value

0.218") and two (0.220") SSs do not differ significantly.

In addition, we compared the spread of pointing points with the calculated error of spacecraft orientation sustaining. The spread of the points characterizes the operation of the spacecraft stabilization system. The spread median values for right ascension and declination are 1.34" (Fig. 6a; 96.6% of data are plotted) and 1.13" (99.8% of data), respectively. These values agree with the calculated upper limit value (2.3").

CONCLUSIONS

(1) SRT pointing in the RadioAstron project is sustained with an accuracy about $\sigma = 0.2''$, which completely meets RSs for scientific observations. In this case, the accuracy of the operation of the orientation-sustaining system is better than 1.4" for about 1 h, which agrees with the calculated values.

(2) The dependence of the pointing accuracy on the number of used SSs was not found. The absence of the restriction to the number of used SSs makes it possible to increase the number of scientific sessions; as a result, the effectiveness of RadioAstron increases.

(3) We measured the systematic deviation (2.5') of the real SRT electric axis from the X axis of the sight coordinate system. It is especially important to take this effect into account when observations are performed in the 1.35-cm band.

ACKNOWLEDGMENTS

This work was supported by the Russian Foundation for Basic Research, project no. 13-02-12103. The

RadioAstron project is led by the Astro Space Center of the Lebedev Physical Institute of the Russian Academy of Sciences and the Lavochkin Scientific and Production Association under a contract with the Russian Federal Space Agency, in collaboration with partner organizations in Russia and other countries.

REFERENCES

1. Kardashev, N.S., Khartov, V.V., et al., RadioAstron—A telescope with a size of 300 000 km: Basic parameters and first results of observations, *Astron. Zh.*, 2013, vol. 90, pp. 179–222.
2. Fedorchuk, S.D. and Arkhipov, M.Yu., Issues of providing for high-precision design of a space radio telescope in the RadioAstron project, *Kosm. Issled.*, 2014, vol. 52, no. 5, pp. 415–417.
3. Voinakov, S.M., Filippova, E.N., Sheikhet, A.I., and Yakimov, V.E., Functional constraints on orientation of onboard and ground-based facilities in the RadioAstron project, *Kosm. Issl.*, 2014, vol. 51, no. 5, pp. 408–414.
4. Avanesov, G.A., et al., Investigation of displacement of the energy center of star images with respect to the geometric center on a CCD matrix and correction of the error of method, in *Sb. tr. vseros. nauch.-tekhn. konf. "Sovremennye problemy opredeleniya orientatsii i navigatsii kosmicheskikh apparatov"* (Proc. of All-Russia Scientific and Engineering Conf. "Modern Problems of Spacecraft Attitude Determination and Navigation"), 2008.

Translated by Yu. Safronov